

A method for locating symmetric homoclinic orbits using symbolic dynamics

This article has been downloaded from IOPscience. Please scroll down to see the full text article.

2000 J. Phys. A: Math. Gen. 33 8059

(<http://iopscience.iop.org/0305-4470/33/45/305>)

View [the table of contents for this issue](#), or go to the [journal homepage](#) for more

Download details:

IP Address: 171.66.16.123

The article was downloaded on 02/06/2010 at 08:35

Please note that [terms and conditions apply](#).

A method for locating symmetric homoclinic orbits using symbolic dynamics

J M Bergamin[†], T Bountis[†] and C Jung[‡]

[†] Department of Mathematics and Centre for Research and Applications of Nonlinear Systems, University of Patras, 26500 Patras, Greece

[‡] Centro de Ciencias Fisicas, Universidad Nacional Autonoma de Mexico, Apartado postal 48-3, 62251 Cuernacava, Mexico

Received 17 July 2000

Abstract. In this paper we present a method which can identify and locate symmetric homoclinic orbits in a homoclinic tangle formed by the intersecting stable and unstable manifolds of a symmetric 2D map. The method consists of a systematic search in parameter space and determination of the order in which these orbits arise using symbolic dynamics. Each orbit corresponds to a unique sequence and it is computed by iterating the map along the unstable manifold to match a specific symmetry at the middle of the orbit. An application of the method to the determination of multibreather solutions of 1D lattices is discussed.

1. Introduction

Finding spatially localized oscillatory solutions in 1D lattices in a systematic way is a topic which has received a lot of attention over the last few years [1–11]. These solutions, often called breathers or multibreathers (depending on the number of spatial extrema), are important in a number of physical and biological applications.

One robust method for finding them was introduced by MacKay and Aubry [12–15] and later developed and used extensively by many researchers (see e.g. [7, 16–21]). It starts from the limit of zero coupling between the particles (the so-called anticontinuum limit) and continues the solution to a situation of nonzero coupling.

As has been discussed by several authors [22–30] the study of (multi)breathers is closely related to the location of homoclinic orbits in maps. The 1D lattice equations are converted into N -dimensional mappings by taking Fourier series or by using Poincaré intersections. In this paper, we examine the case of a 2D map of this type, associated with the following evolution equation for a 1D lattice of identical particles [28]:

$$\ddot{u}_n + V'(u_n) = \alpha(u_{n+1} - 2u_n + u_{n-1}) \quad (1)$$

with

$$V(u_n) = \frac{1}{2}Ku_n^2 + \frac{1}{4}u_n^4 \quad (2)$$

where $u_n = u_n(t)$ is the (real) amplitude of the n th particle. Substituting a Fourier series for u_n and taking into account only the largest Fourier coefficient A_n a 2D mapping is obtained [28]:

$$A_{n+1} + A_{n-1} + CA_n = 3A_n^3 \quad (3)$$

with

$$C = - \left(2 + \frac{K - \omega^2}{\alpha} \right) \quad (4)$$

where ω is the frequency of oscillation of the (multi)breathers. This map has a fixed point at the origin, which for $|C| > 2$ is of the saddle type. Its stable and unstable manifolds intersect and thus a homoclinic tangle is formed. Homoclinic orbits of the mapping are then associated with breather and multibreather solutions of equation (1), the breathers corresponding to one-extremum oscillations of the lattice and the multibreathers to multi-extremum oscillations. There are infinitely many and highly complex multibreather solutions but only a finite number of breather solutions, which are all found with the method described in this paper.

Locating homoclinic orbits of a 2D map can be accomplished following e.g. Beyn and Kleinkauf [31,32], who solve a system of nonlinear equations using Newton's method, starting from some initial guess. In principle, all homoclinic orbits of a system can be found in this way but, without a detailed classification to guide the choice of starting points, the convergence of Newton's scheme is difficult to control.

In this paper, a different way of locating homoclinic orbits is presented. Using the same system of nonlinear equations as Beyn and Kleinkauf, a function is constructed (called here the *matching function*) whose zeros correspond to approximations of homoclinic orbits of the mapping. An advantage of the new method is that it assigns to homoclinic orbits a certain order, thus making the location of a particular homoclinic orbit easy once its order is known.

Using symbolic dynamics to describe the dynamics of mappings in a homoclinic tangle is also a well known approach (see e.g. [35–39]). Applying symbolic dynamics to the simple 2D map described above, we establish an exact correspondence between each homoclinic orbit and the zeros of the matching function. In particular, symbolic dynamics is used to predict the order in which homoclinic orbits are found. Thus, combining these ideas with our matching function we show how a unique classification of homoclinic orbits can be achieved and how each of them can be explicitly computed.

All the homoclinic orbits we obtain are *symmetric* in the sense that the 'left half' of them, from $n = -\infty$ to 0, is identical to the 'right half', according to a reflection ($A_n = A_{-n}$) or anti-reflection ($A_n = -A_{-n}$) symmetry. Currently, we are investigating extensions of our approach to asymmetric homoclinic orbits of (3), which will be presented in a future publication.

Our method for locating the symmetric homoclinic orbits of the mapping (3) consists of the following steps.

- (i) Using the symmetries of the system, certain conditions at the middle of a homoclinic orbit are formulated, which we call the *centre conditions*. When one of them is fulfilled it gives rise to a so-called *matching function*, whose zeros correspond to the homoclinic orbits of the system.
- (ii) A symbolic plane is formed by dividing the space into subregions whose symbolic description is assigned according to the folding of the stable and unstable manifolds.
- (iii) The symmetries of the system give rise to a set of *admissible symbolic sequences*, every one of them being equivalent to a unique homoclinic orbit.
- (iv) Using the dynamics of the map it is then possible to predict the order in which symbolic sequences will occur as the parameter of the system increases.

Step (i) refers to what we call the centre condition method (CCM), (see section 2 below), while steps (ii) and (iii) identify each homoclinic orbit uniquely. Finally, step (iv) provides the bridge between locating and identifying homoclinic orbits by predicting the order of the sequences found in step (i). The combination of the CCM with symbolic dynamics thus gives the desired result.

After the above steps have been completed, a given homoclinic orbit can be found according to the following prescription.

- (i) Choose the desired form of homoclinic orbit (i.e. the number of critical points of large amplitude and their spatial position) and identify its symmetry.
- (ii) Transform this orbit into a symbolic sequence and estimate the number of iterations N required to achieve a desired accuracy ϵ .
- (iii) Locate the desired symbolic sequence in the list of admissible sequences ordered according to the dynamics.
- (iv) Compute the zero of the matching function that corresponds to the desired symbol sequence and use this to obtain an approximation to the homoclinic orbit.

In the next section, the CCM is described and in section 3 it is applied to the example of equation (3). Section 4 gives the symbolic dynamics of this map. In section 5 we combine the results of the previous sections, and we present our conclusions in section 6.

2. The centre condition method

In trying to accurately locate points homoclinic to a saddle equilibrium of a mapping, one usually searches the phase plane of the map for intersections between the stable and unstable manifold. Generally, the simplest way to achieve this is by a shooting strategy: search the plane methodically for points close to the equilibrium lying on an unstable manifold, whose emanating orbit returns to equilibrium after some iterations of the mapping, following the stable manifold [33, 34].

A more advanced method was introduced by Beyn and Kleinkauf [31, 32], who derive a system of N nonlinear equations, and solve it using Newton’s iterative algorithm. In short, one starts with a point close to the unstable manifold and close to equilibrium, and iterates forward this point analytically N times, thus creating a system of N equations. This can be viewed as a boundary condition with the requirement that the end point lie on the stable manifold (and close to the equilibrium) constituting a second boundary condition. By choosing a suitable initial guess for the ‘shape’ of the orbit (which turns out to be quite an arbitrary choice in most cases) a homoclinic orbit can thus be found.

In principle, we shall use the same system of nonlinear equations. However, we will search for a homoclinic orbit not in phase space, but in parameter space. If the mapping depends on a single parameter, we thus search only in a 1D space, even if the mapping is high dimensional. The symmetry condition at the centre is fulfilled for certain values of this parameter. Ordering these parameter values provides a way for ordering the homoclinic orbits as well.

More specifically, consider a general map, depending on a single parameter C :

$$\vec{x}_{n+1} = f(\vec{x}_n; C) \tag{5}$$

having a fixed point $\vec{x} = \vec{\xi}$:

$$f(\vec{\xi}; C) = \vec{\xi} \tag{6}$$

which is a saddle, and proceed as follows.

Suppose \vec{V} is a normalized eigenvector tangent to the unstable manifold of the saddle, depending on the parameter C . Then, introduce the boundary condition

$$\vec{x}_{-N}(C) = \epsilon \vec{V}(C) + \vec{\xi} \quad N \gg 1 \quad 0 < \epsilon \ll 1 \tag{7}$$

approximating the homoclinic orbit at minus infinity. Applying the map (5) N times to $\vec{x}_{-N}(C)$ gives the vector $\vec{x}_0(C)$, whose value thus depends on C (we call this C the *independent* parameter C_1).

Now suppose this new vector $\vec{x}_0(C)$ satisfies some symmetry condition (the ‘centre condition’) about the central point, for a general value of the parameter C of the map. Use this condition to obtain an additional expression for the orbit, and call its *dependent* parameter $C = C_D$. Now, we have C_D as a function of C_1 . Then, the zeros of the matching function

$$M(C_1) = C_D(C_1) - C_1 = 0 \quad (8)$$

correspond to homoclinic orbits of the map (5).

3. Application to a simple 2D map

To illustrate this method, let us consider a simple 2D map, obtained from a truncated Fourier series description of a 1D chain of oscillators [28], as described in section 1:

$$T : \begin{cases} A_{n+1} = 3A_n^3 - CA_n - B_n \\ B_{n+1} = A_n. \end{cases} \quad (9)$$

This map has a saddle fixed point at the origin, with the normalized stable and unstable eigenvectors given respectively by

$$\vec{V}_S = \pm \frac{1}{\sqrt{\lambda_+^2 + 1}} \begin{pmatrix} \lambda_+ \\ 1 \end{pmatrix} \quad \vec{V}_U = \pm \frac{1}{\sqrt{\lambda_-^2 + 1}} \begin{pmatrix} \lambda_- \\ 1 \end{pmatrix} \quad (10)$$

where

$$\lambda_{\pm} = \frac{-C \pm \sqrt{C^2 - 4}}{2} \quad (11)$$

are the eigenvalues of the map (9) linearized about $A_n = B_n = 0$. In figure 1 we plot the first part of the stable and unstable manifolds emanating from the origin. The intersections of these manifolds correspond to homoclinic orbits.

Note that T is symmetric with respect to the lines $B_n = \pm A_n$. These symmetries give rise to four centre conditions, each providing a necessary condition for a particular homoclinic orbit to exist:

$$A_{-1} = \pm A_1 \quad \text{giving} \quad A_{-n} = \pm A_n \quad \forall n \in N \quad (12)$$

$$A_0 = \pm A_1 \quad \text{giving} \quad A_{-n+1} = \pm A_n \quad \forall n \in N. \quad (13)$$

In figure 2, we sketch the shapes of the simplest homoclinic orbits corresponding to these conditions. Inserting (12) and (13) in the mapping T , we find the following equations for the parameter C_D :

$$A_{-1} = A_1 : C_D = 3A_0^2 - 2\frac{A_{-1}}{A_0} \quad \text{centre condition 1} \quad (14)$$

$$A_{-1} = -A_1 : C_D = 3A_{-1}^2 - \frac{A_{-2}}{A_{-1}} \quad \text{centre condition 2} \quad (15)$$

$$A_0 = A_1 : C_D = 3A_0^2 - \frac{A_{-1}}{A_0} - 1 \quad \text{centre condition 3} \quad (16)$$

$$A_0 = -A_1 : C_D = 3A_0^2 - \frac{A_{-1}}{A_0} + 1 \quad \text{centre condition 4.} \quad (17)$$

Observe that equation (15) is applied to the vector (A_{-2}, A_{-1}) since $A_0 = 0$ and thus a unique equation cannot be formulated using a vector depending on A_0 .

Using centre condition 1 (14), a value for ϵ , $\epsilon = 10^{-18}$, and the mapping (9), homoclinic orbits have been located. Table 1 gives the results for $2N + 1 = 33, 35, 37, 39$ and 41 particles.

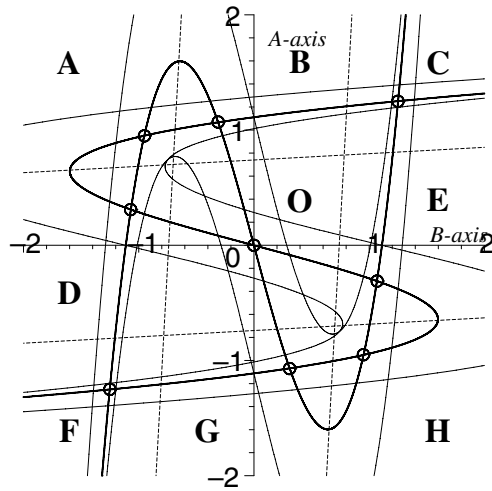


Figure 1. The first part of the stable and unstable manifolds of the mapping (9) (solid curves). Points where these manifolds intersect are homoclinic points, i.e. each generates a homoclinic orbit when it is iterated forward and backward using the mapping (9) and its inverse. The circles indicate the first primary intersection points (FPIPs), (see text). The symbols A, B etc indicate the nine regions of the symbolic plane, approximately delimited by the dashed lines.

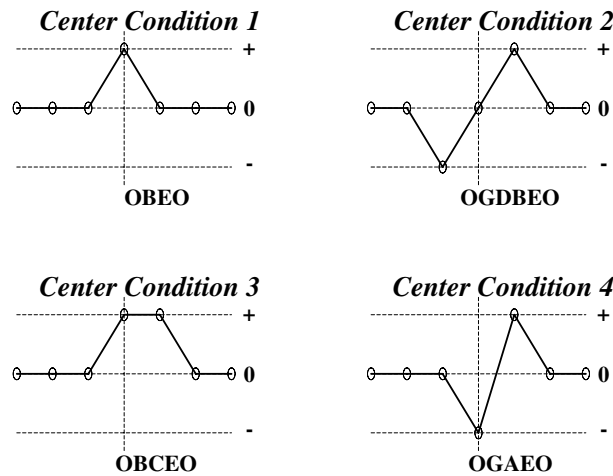


Figure 2. Simple examples of the kind of homoclinic orbit corresponding to each of the centre conditions (14)–(17). Given here is a schematic representation, with only three possible values for the amplitudes: 0, + and –. Using these, a translation to the symbolic plane is made by taking each symbol and its successor and combining them into one symbol (see the text). For instance, the sequence 00 + 00 becomes (00)(0+)(+0)(00), which is equivalent to OBEO.

The number of such orbits computed by the matching function (8) respectively is $3^0 = 1$, $3^1 = 3$, $3^2 = 9$, $3^3 = 27$ and $3^4 = 81$ respectively.

We must mention here the fact that increasing ϵ , increasing C or increasing N have similar effects: a scaling arises which repeats (and extends) the sequence of zeros again and again for higher C -values when ϵ and N are kept constant. Therefore, we have to restrict our parameter

Table 1. Zeros of the matching function (8) for the mapping (9) with $\epsilon = 10^{-18}$.

$N = 16$	C	16	14.066 209 09	20	12.016 222 67	52	14.068 527 71
1	14.068 703 62	17	14.066 388 42	21	12.016 430 77	53	14.068 539 94
$N = 17$	C	18	14.068 534 42	22	12.044 639 10	54	14.068 691 56
1	12.013 731 91	19	14.068 872 19	23	12.044 7 416 1	55	14.068 715 69
2	14.038 837 03	20	14.070 962 84	24	12.045 495 85	56	14.068 866 67
3	14.103 271 80	21	14.071 124 76	25	12.045 660 83	57	14.068 878 75
$N = 18$	C	22	14.101 418 63	26	12.046 586 56	58	14.070 955 44
1	10.452 112 98	23	14.101 498 14	27	12.046 611 21	59	14.070 962 68
2	11.986 110 62	24	14.102 241 74	28	14.035 766 50	60	14.071 030 35
3	12.011 049 12	25	14.102 373 33	29	14.035 769 03	61	14.071 042 20
4	14.035 769 09	26	14.103 248 28	30	14.035 811 04	62	14.071 120 13
5	14.038 774 37	27	14.103 300 82	31	14.035 817 39	63	14.071 124 83
6	14.066 313 62	$N = 20$	C	32	14.035 855 66	64	14.101 418 56
7	14.071 042 18	1	8.273 178 57	33	14.035 856 88	65	14.101 420 83
8	14.101 501 68	2	9.213 532 27	34	14.037 277 66	66	14.101 458 56
9	14.103 300 80	3	9.234 029 56	35	14.037 285 23	67	14.101 464 34
$N = 19$	C	4	10.422 419 30	36	14.037 382 51	68	14.101 498 13
1	9.237 291 69	5	10.426 394 37	37	14.037 398 24	69	14.101 501 73
2	10.426 514 46	6	10.449 158 89	38	14.037 497 84	70	14.102 241 73
3	10.483 530 62	7	10.454 948 31	39	14.037 506 16	71	14.102 243 81
4	11.982 545 53	8	10.481 592 11	40	14.038 768 05	72	14.102 303 44
5	11.986 022 69	9	10.483 572 75	41	14.038 774 24	73	14.102 312 81
6	12.011 059 68	10	11.982 541 67	42	14.038 832 00	74	14.102 371 12
7	12.016 324 18	11	11.982 654 37	43	14.038 841 97	75	14.102 375 62
8	12.044 747 21	12	11.984 293 53	44	14.038 906 82	76	14.103 245 86
9	12.046 649 65	13	11.984 594 25	45	14.038 910 74	77	14.103 248 17
10	14.035 766 50	14	11.986 022 42	46	14.066 209 00	78	14.103 269 86
11	14.035 852 87	15	11.986 216 58	47	14.066 214 21	79	14.103 273 71
12	14.037 281 53	16	12.010 916 05	48	14.066 300 48	80	14.103 299 29
13	14.037 501 32	17	12.011 156 06	49	14.066 313 60	81	14.103 300 82
14	14.038 774 24	18	12.013 510 66	50	14.066 393 82		
15	14.038 910 62	19	12.013 951 80	51	14.066 396 58		

space. We want to find orbits with low C -values and have chosen N and ϵ in such a way that when we restrict the parameter space to $2 \leq C \leq 15$ the first zero of the matching function will arise for $N = 16$. The reason for this choice is purely for numerical convenience.

4. Symbolic dynamics

Symbolic dynamics can be used to describe different types of orbit of a nonlinear system. Hao and Zheng give a complete theory in their book [36] while Jung and co-workers use it to study the dynamics of escape orbits in two-degrees-of-freedom Hamiltonian systems [37–39]. Here, we follow a simple approach to generate a symbolic plane and study the dynamics on this plane.

Looking at the intersection points of the manifolds of the mapping (5) we notice in figure 1 nine regions of high activity. These regions are found around the FIPs of the manifolds: they are the origin and the eight points corresponding to the highest amplitudes of the simplest type of homoclinic orbit, namely those making only one excursion from the origin. We thus divide the phase space into nine regions, forming a partition which generates the symbolic dynamics.

Observe in figure 2 that (in a symbolic language) there are three ‘levels’ among which

Table 2. The order in which successive symbols can occur in one sequence.

After the symbol	Follows
A, B or C	C, E or H
D, O or E	B, O or G
F, G or H	A, D or F

Table 3. Negative and inverse of each symbol.

Symbol	Has negative	And inverse
A	H	H
B	G	E
C	F	C
D	E	G
O	O	O
E	D	B
F	C	F
G	B	D
H	A	A

the amplitudes of the homoclinic orbits alternate: 0, + and -. These three symbols can be combined in nine pairs which are assigned to the nine regions of figure 1 as follows: A to (-+), B to (0+), C to (++), D to (-0), O to (00), E to (+0), F to (--), G to (0-) and H to (+-).

Now, using our mapping T , (9), we can determine a set of simple rules which successive symbols must obey following the iteration of points by the map: since we plot coordinates (A_n, A_{n+1}) in figure 1, this means that the point $(B_n, A_n) = (A_{n-1}, A_n)$ is mapped under T into $(B_{n+1}, A_{n+1}) = (A_n, A_{n+1})$, hence the vertical coordinate of the n th point becomes the horizontal one of the $(n + 1)$ th. This implies that the A, B and C regions of the plane are mapped to any one of the C, E or H regions, the D, O, E regions to either B, O or G and the F, G, H regions to either A, D or F, as shown in table 2.

The reader can easily verify, plotting schematically homoclinic orbits as arrays of particles in a 1D lattice, that the rules of table 2 give the only possible ways for connecting successive particles from levels 0, + or - to the next level (see figure 2).

Observe now that in the symbolic language introduced above, a homoclinic orbit begins and ends with an infinite number of O and has in its central part only a finite number of symbols different from O. Thus, a homoclinic sequence of length k can be defined as a finite sequence with k symbols whose first and last symbols are O and whose second and second-to-last symbols are not O. The smallest symbolic sequences corresponding to a homoclinic orbit of our map are thus four symbols long and according to the rules in table 2 are OBEO and OGDO (each other's negative equivalent).

Furthermore, all the orbits obtained by the CCM, iterating T from $n = -N$ forward to 0, possess either an even or an odd symmetry. This means that a solution followed further from $n = 0$ to N will be either the negative equivalent (the sign of all amplitudes changes) or the same as the original solution. In terms of a symbolic sequence, this rule necessitates that the sequence of the 'backward' orbit (followed by T^{-1} from $n = 0$ to $-N$) will be either the inverse or the negative inverse of the original sequence. The inverse and negative of each symbol are given in table 3.

Thus, we can construct in a systematic way all homoclinic orbits possessing these

Table 4. All possible symmetric homoclinic orbits with maximum length 8 and the centre condition by which they are found. The vertical axis gives the first half sequence, the horizontal axis the second half sequence. The numbers in the table refer to which centre condition is fulfilled, see the text, equations (14)–(17).

		O																		
		D								O				E						
		F	G	H	D	O	E	A	B	C	F	G	H	D	O	E	A	B	C	
		F	G	H	D	O	E	A	B	C	F	G	H	D	O	E	A	B	C	
	C																		3	1
	C E	2																		1
	H										4									1
	B																			1
B	E O				2															1
	G																		1	
	A										4								1	
	H D				2														1	
	F																		3	1
	C	4																	3	1
	B E										2								1	
	H											4							1	3
	B												4						1	3
O	O O																			
	G										3								1	4
	A											3							1	4
	G D																		1	2
	F	3																	1	3
	C																		1	3
	A E																		1	2
	H																		1	4
	B																		1	
G	D O																		1	2
	G																		1	
	A																		1	4
	F D	1																	1	2
	F	1																	1	3

symmetries. In table 4 we list all possible sequences involving combinations of up to eight symbols. The admissible ones among them (i.e. those following the rules of tables 2 and 3) are designated by a number in their entry which corresponds to the number of the centre condition by which they are found (see equations (14)–(17)). Empty entries correspond to either non-admissible or non-symmetric orbits.

Now we are ready to combine the results of the CCM with symbolic dynamics to explain how each zero of the matching function (8) can be identified with a unique symbolic sequence

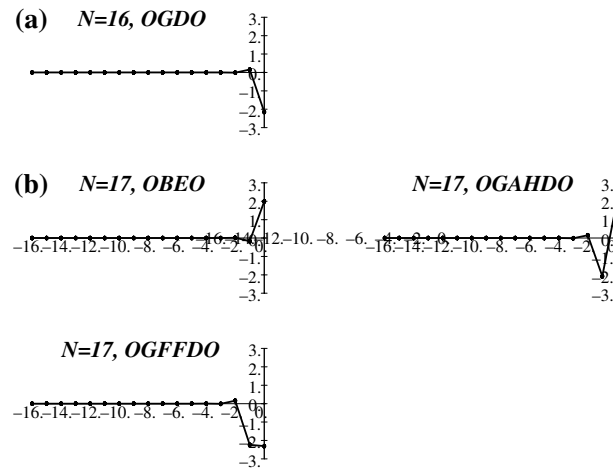


Figure 3. Homoclinic orbits found using the CCM for the mapping (9). Since $B_{n+1} = A_n$ only the A_n are plotted. Because of symmetry, only the first half of the orbit is given. The horizontal axis denotes the position n , the vertical axis the amplitude A_n . (a) The only orbit found for $N = 16$ and $\epsilon = 10^{-18}$. Symbolic sequence: OGDO. (b) The three orbits found for $N = 17$ and $\epsilon = 10^{-18}$. Symbolic sequences in order of increasing C : OBEO, OGAHDO and OGFFDO.

possessing an even or odd symmetry.

5. Combination of CCM and symbolic dynamics

We will illustrate our approach for the case of even symmetry and, in particular, for the orbits obeying centre condition 1. Their C values are listed in increasing order in table 1, computed as zeros of the matching function (8), for $2N + 1$ sites, $N = 16-19$ and initial condition accuracy $\epsilon = 10^{-18}$.

Let us start first with the case $N = 16$, where only one homoclinic orbit is found at $C = 14.068\ 703\ 62$. It is the simplest one in this category, described by the symbolic sequence OBEO. Decreasing the value of N and keeping the same ϵ -accuracy yields no homoclinic orbits as the number of iterations is too small and the accuracy too demanding. In figure 3(a), we have plotted the left-hand half of this orbit, obtained as a zero of the matching function in the form OGDO (the negative equivalent of OBEO).

For $N = 17$, the three homoclinic orbits computed by (8) are plotted in figure 3(b) in the following order of decreasing C values:

$$\text{OGFFDO}, \quad \text{OGAHDO} \quad \text{and} \quad \text{OBEO} \quad (\text{negative of OGDO}). \quad (18)$$

Let us now define an order of *dynamic sequencing*. We do this by giving the order of how a sequence can change as C is decreased. Furthermore, we follow an approach which preserves the main part of the sequence by changing the middle symbols first, since this modifies only one or two symbols of the sequence at a time. Because of the even or odd symmetry it suffices to work with *left half sequences* only. The shortest such sequence is therefore OB (or OG, its negative equivalent).

Each symbol changes into its dynamic predecessor, as follows. All ‘amplitudes’ A_n are continuous functions of the map parameter C . If (A_n, A_{n+1}) is on the unstable manifold, increasing C will move this coordinate along the manifold in the direction away from the origin (measured along the manifold). If (A_n, A_{n+1}) is in O, on the part of the unstable

Table 5. The dynamic predecessors of each symbol.

Symbol	Has dynamic predecessors
A	D and B
B	A and O
C	C and E
D	F and A
O	B and G
E	C and H
F	F and D
G	H and O
H	E and G

manifold emerging directly from the origin, increasing C can cause it to move to either B or G (see figure 1). Thus, O is one of the predecessors of B and G. From B, (A_n, A_{n+1}) can move to A, then to D and F, following the unstable manifold, as we increase C . This manifold turns around in F, so from F the coordinate pair can now move back successively to D, A, B and O. From this, one sees that A is also a predecessor of B. Thus, B has two dynamic predecessors: O and A. Starting again from the origin and following the unstable manifold into G (as C increases) and then through H, E and C we finally obtain the full list of dynamic predecessors appearing in table 5.

Thus, we find that the sequence OB is indeed the sequence corresponding to the lowest C value: the dynamic predecessor of B is either A or O. However, A gives the non-admissible sequence OAHO (see table 2) and O gives the ‘trivial’ homoclinic orbit OOOO. Hence, there is no sequence with a lower C value than OB.

The half sequence of length k corresponding to the highest C value is the one starting with OG followed by $k - 2$ times the symbol F (or the negative version OB followed by Cs). This is because this sequence is not the predecessor of any other sequence of length k , but has many predecessors, starting with OGF...FD. Since a predecessor has a lower C value, we must conclude that OGF...FF has to be the sequence with the highest C value.

As an example, let us construct the complete set from the sequence OGFFFFDO, whose half-sequence is $S_1 = OGFF$. Its predecessors are OGFF and OGFD. Now, OGFF is the same as the original and will thus not decrease the C value, so we write $S_2 = OGFD$, whose predecessors are OGFF and OGFA. OGFF is S_1 so S_3 has to be OGFA, with OGFB as its possible predecessor. However, according to the rules in table 2 this sequence is not admitted. From here on, since we cannot continue with just changing the rightmost symbol, we have to change also its neighbour to the left.

We keep again as many as possible symbols the same, so from $S_3 = OGFA$ we go to OGDA. However, this gives a non-admissible solution, so we try the predecessors of A: OGDD and OGDB. The first is not admitted, so $S_4 = OGDB$. Continuing in this way, we find $S_5 = OGDO$, $S_6 = OGDG$, $S_7 = OGAH$, $S_8 = OGAE$ and $S_9 = OGAC$.

The predecessor of S_9 is OABC since OO cannot be followed by an A. So $S_{10} = OABC$, $S_{11} = OOBE$, $S_{12} = OOBH$ and finally $S_{13} = OOOG$, the shortest possible sequence, having the lowest C value.

Symbolic dynamics thus predicts 13 homoclinic orbits. With the CCM and $N = 18$ however, we found only nine, all of which are present in the above list of sequences and in the right order. What about the missing four orbits? If we look at the homoclinic orbits found by the CCM with $N = 19$ we see again nine homoclinic orbits with length $k = 4$, thus again missing four orbits. However, these missing orbits are *different* from the ones missing at

$N = 18$. Combining all orbits of length 4 from $N = 18$ and 19, we thus obtain the complete set of 13 orbits, in the right order.

For $N = 20$ again four orbits are missing from those with four symbols but they are the same as for $N = 18$. This type of alternating appearance and disappearance of k -symbol sequences as N is increased is observed for all the k values we have studied. Thus, if we want to find the full set of homoclinic orbits, we have look at the CCM for a certain N high enough and also at the CCM with $N + 1$ elements. An explanation for this behaviour remains to be found.

As we have demonstrated, however, our approach is systematic and appears to construct all symmetric homoclinic orbits in a prescribed order, as the parameter of our 2D mapping is decreased.

6. Concluding remarks

Localized oscillatory solutions called (multi)breathers of 1D nonlinear lattices have attracted much attention, due to their interesting mathematical properties and potentially relevant physical applications. These solutions have been directly related to the homoclinic orbits of higher-dimensional maps (obeyed by their Fourier coefficients) and their approximation has been shown to be successfully achieved by the computation of homoclinic orbits of as simple a system as a 2D area-preserving map.

In this paper, we have introduced the CCM, combining symmetry properties with symbolic dynamics, to locate and identify all symmetric homoclinic orbits of one such area-preserving 2D map (9), describing multibreather solutions of the 1D lattice (1) and (2). We have found that each homoclinic orbit corresponds to a unique symbolic sequence and that there exists a type of sequencing which predicts the order in which homoclinic orbits are found as a parameter C of the map is varied.

One rather inconvenient aspect of our approach is that we cannot directly specify a certain value of C and find a symmetric homoclinic orbit present at this value. However, changing the accuracy parameter ϵ of the CCM, the zeros of the matching function change smoothly until each of them ceases to exist. Thus, when one has found a zero at a certain value of C , one can in principle move this zero to any desired value of C , by changing the parameters of the CCM accordingly.

Finally, as described in this paper, our method is applicable to any 2D area-preserving map which depends on a single parameter. Work is currently under way to extend this approach so that it can be applied to more general 2D maps and also to mappings with higher dimensions and more parameters.

In this paper we have described an approach for finding symmetric and antisymmetric homoclinic orbits of a cubic 2D map. One way to find the asymmetric ones is by adding and subtracting our 2D mapping with its inverse. Clearly, the symmetric (and antisymmetric) homoclinic orbits of the resulting 4D map would thus yield all (including asymmetric) homoclinic orbits of the original 2D map. We have already started working in this direction and results will appear in a future publication.

Acknowledgments

We are grateful to P Panayotaros for some discussions on this subject. One of us (TB) is grateful for the hospitality of the Centro Internacional de Ciencias of Cuernacava, Mexico, where part of this work was completed. We also acknowledge the support of the 'Karatheodory' programme

of the Department of Mathematics of the University of Patras and a PENED grant no 99–146 from the GSRT of the Greek Ministry of Development.

References

- [1] Hennig D and Tsironis G 1999 *Phys. Rep.* **307** 333
- [2] Sievers A J and Takeno S 1988 *Phys. Rev. Lett.* **61** 970
- [3] Takeno S and Homma S 1991 *J. Phys. Soc. Japan* **60** 73
- [4] Takeno S 1992 *J. Phys. Soc. Japan* **61** 2821
- [5] Takeno S and Homma S 1993 *J. Phys. Soc. Japan* **62** 835
- [6] Segur H and Kruskal M D 1987 *Phys. Rev. Lett.* **58** 747
- [7] Bambusi D 1996 *Nonlinearity* **9** 433
- [8] Takeno S and Peyrard M 1996 *Physica D* **92** 140
- [9] Bikaki A, Voulgarakis N K, Aubry S and Tsironis G P 1999 *Phys. Rev. E* **59** 1234
- [10] Balmforth N J, Craster N V and Kevrekidis P G 2000 *Physica D* **135** 212
- [11] Kopidakis G and Aubry S 1999 *Physica D* **130** 155
- [12] MacKay R S and Aubry S 1994 *Nonlinearity* **7** 1623
- [13] MacKay R S 1995 *Physica D* **86** 122
- [14] Aubry S 1995 *Physica D* **86** 284
- [15] Aubry S 1994 *Physica D* **71** 196
- [16] Aubry S 1997 *Physica D* **103** 201
- [17] Marin J L and Aubry S 1996 *Nonlinearity* **9** 1501
- [18] Marin J L, Aubry S and Floria S 1998 *Physica D* **113** 283
- [19] Aubry S and Creteigny T 1998 *Physica D* **119** 34
- [20] Hornquist M, Lennholm E and Basu C 2000 *Physica D* **136** 93
- [21] Marin J L and Aubry S 1998 *Physica D* **119** 163
- [22] Flach S 1994 *Phys. Rev. E* **50** 3134
- [23] Flach S 1995 *Phys. Rev. E* **51** 1504
- [24] Flach S and Willis C R 1998 *Phys. Rep.* **295** 181
- [25] Hennig D, Rasmussen K O, Gabriel H and Bülow A 1996 *Phys. Rev. E* **54** 5788
- [26] Kollmann M and Bountis T 1998 *Physica D* **113** 397
- [27] Kollmann M, Capel H W and Bountis T 1999 *Phys. Rev. E* **60** 1195
- [28] Bountis T, Capel H W, Kollmann M, Ross J C, Bergamin J M and Van der Weele J P 2000 *Phys. Lett. A* **268** 50
- [29] Flach S 1995 *Phys. Rev. E* **51** 3579
- [30] Bülow A, Hennig D and Gabriel H 1999 *Phys. Rev. E* **59** 2380
- [31] Beyn W-J and Kleinkauf J-M 1997 *SIAM J. Numer. Anal.* **34** 1207
- [32] Beyn W-J and Kleinkauf J-M 1997 *Numer. Algorithms* **14** 25
- [33] Friedman M J and Doedel E J 1991 *SIAM J. Numer. Anal.* **28** 789
- [34] Farantos S 1998 *Comput. Phys. Commun.* **108** 240
- [35] Fang H P 1994 *J. Phys. A: Math. Gen.* **27** 5187
- [36] Hao B-L and Zheng W-M 1998 *Applied Symbolic Dynamics and Chaos* (Singapore: World Scientific)
- [37] Ruckerl B and Jung C 1994 *J. Phys. A: Math. Gen.* **27** 55
- [38] Ruckerl B and Jung C 1994 *J. Phys. A: Math. Gen.* **27** 6741
- [39] Jung C, Lipp C and Seligman T H 1999 *Ann. Phys., NY* **275** 151